TOPOLOGICAL DERIVATIVE-BASED TOPOLOGY OPTIMIZATION OF STRUCTURES SUBJECT TO SELF-WEIGHT LOADING

A.A. NOVOTNY, C.G. LOPES AND R.B. SANTOS

Abstract. Topology optimization of structures subject to self-weight loading has received considerable attention in the last decades. However, by using standard formulations based on compliance minimization under volume constraint, several difficulties arise once the self-weight of the structure becomes dominant, including non-monotonic behavior of the compliance, possible unconstrained character of the optimum, and parasitic effects for low densities when using density-based methods. In order to overcome such difficulties, a regularized formulation that allows for imposing any feasible volume constraint is proposed. The standard formulation based on compliance minimization under volume constraint is recovered when the regularizing parameter vanishes. The resulting topology optimization problem is solved with the help of the topological derivative method leading to a 0-1 topology design algorithm, which seems to be crucial when the self-weight loading is dominant. Finally, several numerical experiments are presented, showing the effectiveness of the proposed approach in solving a structural topology optimization problem under self-weight loading.

1. Introduction

Structural topology optimization under self-weight loading is a challenging problem, as pointed out in Bruyneel and Duysinx (2005) paper. In particular, by using standard formulations based on compliance minimization under volume constraint, several difficulties arise once the structure's self-weight becomes dominant. The non-monotonic behavior of the compliance, possible unconstrained character of the optimum, and parasitic effects for low densities when using density-based methods. Over the years, several researchers addressed the compliance minimization problem with self-weight loads and sought to overcome the difficulties pointed out by Bruyneel and Duysinx (2005). See also earlier work by Turteltaub and Washabaugh (1999) and recent papers (Xu et al., 2013; Holmberg et al., 2015; Félix et al., 2020). Many approaches have been proposed, such as the use of mathematical programming, heuristics methods, and optimization criteria method (Ansola et al., 2006; Huang and Xie, 2011; Xu et al., 2013). To introduce these ideas, we present a simple example into one spatial dimension.

Example 1. *Let us consider the following boundary value problem modeling an elastic bar submitted to self-weight b and traction q:*

$$\begin{cases} -(\rho u')' = (1-\kappa)\rho b, \quad \text{in } (0,1), \\ u(0) = 0, \quad \rho u'(1) = \kappa q, \end{cases} \tag{1.1}$$

with $0 \leq \kappa \leq 1$. Assuming constant thickness $\rho \in \mathbb{R}^+$, we want to solve the minimization problem:

$$\underset{\rho \in \mathbb{R}^+}{\text{Minimize}}\, C(\rho), \tag{1.2}$$

Date: March 15, 2021.

Key words and phrases. Structural topology optimization, self-weight loading, topological derivative method.

where the compliance $C(\rho)$ is given by

$$\begin{aligned} C(\rho) &= \kappa q u(1) + (1-\kappa)\int_0^1 \rho b u \, dx \\ &= \frac{1}{3}(1-\kappa)^2 \rho b^2 + \frac{1}{\rho}\kappa^2 q^2 + \kappa(1-\kappa) b q. \end{aligned} \tag{1.3}$$

Three cases of interest are considered, namely: $\kappa = 0$, $0 < \kappa < 1$ and $\kappa = 1$. By fixing $b = 10$ and $q = 1$, Figure 1 shows the behavior of the compliance function associated with each case.

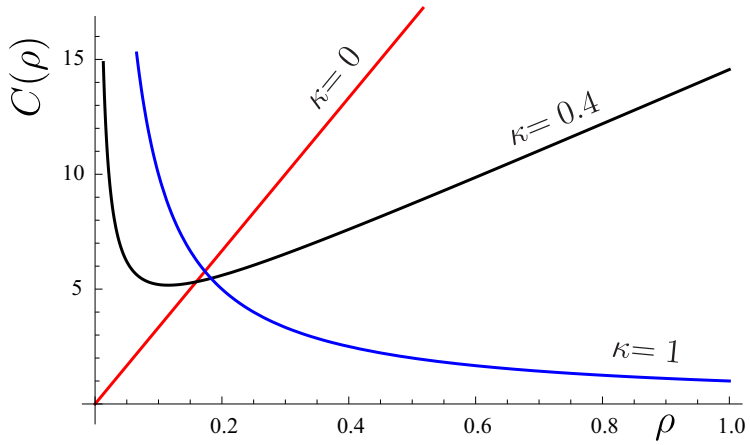

FIGURE 1. Compliance behavior associated with different values of κ.

As a conclusion, three optimal solutions $\rho^\star$ for problem (1.2) can be found, which are:

(1) *When $\kappa = 0$, $\rho^\star$ goes to zero;*
(2) *When $\kappa = 1$, $\rho^\star$ goes to infinity;*
(3) *For $0 < \kappa < 1$ a non-trivial solution $\rho^\star$ can be found.*

Therefore, in order to deal with the case in which the self-weight loading is dominant, let us introduce the following regularized formulation

$$\underset{\rho \in \mathbb{R}^+}{\text{Minimize}}\ F^\alpha(\rho) := C(\rho) + \alpha V(\rho)^{-1}, \tag{1.4}$$

with $0 \leq \alpha < \infty$ representing the regularizing parameter. In the above problem $V(\rho) = \int_0^1 \rho dx = \rho$, since ρ is assumed to be constant. Now, let us set $b = 1$ and $\kappa = 0$ (or $q = 0$). After varying $\alpha = 0, 1, 2, 4, 8, 16$ $(\times 10^{-3})$, the behavior of the regularized function $F^\alpha(\rho)$ can be seen in Figure 2. In this case, a family of non-trivial solutions depending on the penalty parameters $\alpha > 0$ can be found. Note that after reformulating the optimization problem according to (1.4), the resulting formulation for $\alpha > 0$ and $\kappa = 0$ enjoys the same mathematical properties as the compliance function (1.2) for $0 < \kappa \leq 1$. Finally, the original formulation (1.2) is recovered from (1.4) by setting $\alpha = 0$.

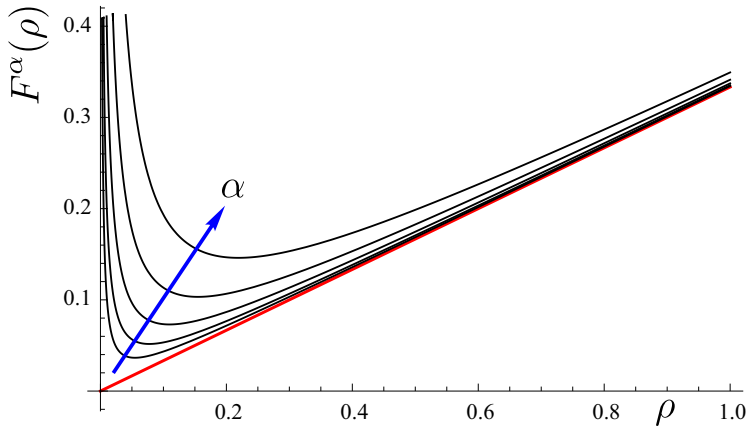

FIGURE 2. Regularized function behavior depending on the values of α.

Despite the intensive research over the past two decades, this subject of matter still requires investigation. Thus, in this paper, the topology optimization of structures subject to self-weight loads is revisited. From the discussion presented in Example 1, a regularized formulation of the compliance-based minimization problem that allows for imposing any feasible volume constraint is introduced. The original formulation is recovered once the regularizing parameter vanishes. The resulting topology optimization problem is solved with the help of the topological derivative method, leading to a 0-1 topology design algorithm. In contrast to traditional topology optimization methods, the topological derivative formulation does not require any material model concept based on intermediary densities, so that the obtained solutions are naturally of the black-white type with no need of post-processing of any kind. This feature seems to be crucial to properly deal with the cases in which the self-weight loading is dominant.

The paper is organized as follows. A regularized formulation inspired by the problem (1.4) is proposed in Section 2, which allows for imposing any feasible volume constraint. The associated topology optimization problem is solved with the help of the topological derivative method in Section 3. The resulting topology design algorithm is presented in Section 4, together with several numerical experiments showing the effectiveness of the proposed approach in different scenarios. Finally, the paper ends with some concluding remarks in Section 5.

2. Problem formulation

Let us consider an open and bounded domain $\mathcal{D} \subset \mathbb{R}^2$, with Lipschitz boundary denoted as $\Gamma := \partial\mathcal{D}$. The boundary Γ is the union of two given non-overlapping subsets, namely, Γ_D and Γ_N. On Γ_D the displacements are prescribed, whereas the boundary tractions are prescribed on Γ_N.

Based on the discussion presented in the simple Example 1, let us consider the following topology optimization problem:

$$\begin{cases} \underset{\Omega\subset\mathcal{D}}{\text{Minimize}}\ \mathcal{F}^\alpha(u) := \mathcal{C}(u) + \alpha|\Omega|^{-1}, \\ \text{Subject to } |\Omega| \leq M, \end{cases} \tag{2.1}$$

where Ω represents the design domain, with $|\Omega|$ used to denote the Lebesgue measure of Ω, i.e. the current volume of the structure. In addition, the quantity $M > 0$ is the volume constraint, $0 \leq \alpha < \infty$ is the regularizing parameter and $\mathcal{C}(u)$ is the structural

compliance, namely

$$\mathcal{C}(u) := \int_{\Gamma_N} q \cdot u \, d\Gamma + \int_{\mathcal{D}} b \cdot u \, d\mathcal{D}, \tag{2.2}$$

with u solution to:

$$\left\{ \begin{array}{rcll} -\text{div}\sigma(u) & = & b & \text{in } \mathcal{D}, \\ u & = & 0 & \text{on } \Gamma_D, \\ \sigma(u)n & = & q & \text{on } \Gamma_N. \end{array} \right. \tag{2.3}$$

The stress tensor $\sigma(u)$ and self-weight b are given, respectively, by:

$$\sigma(u) = \gamma \mathbb{C} \varepsilon(u), \quad b = \gamma b_0, \tag{2.4}$$

with the linearized Green tensor defined as follows

$$\varepsilon(u) = \frac{1}{2}(\nabla u + (\nabla u)^\top). \tag{2.5}$$

The elasticity tensor is written as

$$\mathbb{C} = 2\mu \mathbb{I} + \lambda(\mathrm{I} \otimes \mathrm{I}), \tag{2.6}$$

in which μ and λ are the Lamé's coefficients, both considered constants everywhere. In addition, $\mathbb{I}$ and I are the fourth and the second order identity tensors, respectively. The statement of the problem is complemented with the definition of a piecewise constant function γ, such that:

$$\gamma(x) := \left\{ \begin{array}{ll} 1, & \text{if } x \in \Omega, \\ \gamma_0, & \text{if } x \in \mathcal{D} \setminus \overline{\Omega}, \end{array} \right. \tag{2.7}$$

where $\overline{\Omega}$ is the closure of Ω and $0 < \gamma_0 \ll 1$ is used to mimic voids.

3. Topology optimization method

In this paper, the topological derivative method is used for solving the optimization problem (2.1). The topological derivative is defined as the first term (correction) of the asymptotic expansion of a given shape functional with respect to a small parameter that measures the size of singular domain perturbations, such as holes, inclusions, defects, source-terms, and cracks (Novotny and Sokołowski, 2013). This concept can naturally be used as a steepest-descent direction in an optimization process like in any method based on the gradient of the cost functional. Therefore, the topological derivative concept has applications in many different fields such as shape and topology optimization, inverse problems, imaging processing, multi-scale material design, and mechanical modeling including damage, fracture evolution phenomena, and control of cracks propagation. See, for instance, the book by Novotny et al. (2019).

For the sake of completeness, the topological derivative associated with the shape functional $\mathcal{F}^\alpha(u)$ from (2.1) is stated in its closed form. Since we are using a very compliant material to mimic voids, the topological derivatives are presented in their limit cases versions when a small portion of material is either removed or added to the design domain Ω. Finally, the results are written in terms of the Lamé's coefficients, so that they can be used either in plane stress or plane strain assumptions.

Theorem 2. *The topological derivatives of the shape functional $\mathcal{F}^\alpha(u)$ from (2.1), with respect to the nucleation of a small circular inclusion endowed with different material property from the background, is given by*

$$D_T \mathcal{F}^\alpha(x) = D_T \mathcal{C}(x) - \alpha |\Omega|^{-2} D_T |\Omega|(x), \quad \forall x \in \mathcal{D}. \tag{3.1}$$

See, for instance, the book by (Novotny and Sokołowski, 2020, Ch. 5). We are interested into two particular cases, which are:

Case 1. *Let us consider $x \in \Omega$. In this case $\gamma = 1$ and a small portion of material is removed. Then the topological derivative $D_T\mathcal{C}$ of the compliance functional reads*

$$D_T\mathcal{C} = \mathbb{P}_0\sigma(u) \cdot \varepsilon(u) - 2b_0 \cdot u, \tag{3.2}$$

where the displacement u is solution to (2.3) and the polarization tensor $\mathbb{P}_0$ is written as

$$\mathbb{P}_0 = \frac{\lambda + 2\mu}{\lambda + \mu}\left(2\mathbb{I} - \frac{\mu - \lambda}{2\mu}\mathrm{I} \otimes \mathrm{I}\right). \tag{3.3}$$

Finally, the topological derivative $D_T|\Omega|$ is given by

$$D_T|\Omega| = -1. \tag{3.4}$$

Case 2. *Now, let us consider $x \in \mathcal{D} \setminus \overline{\Omega}$. In this case $\gamma = \gamma_0 \ll 1$ and a small portion of material is added. Then the topological derivative $D_T\mathcal{C}$ can be written as*

$$D_T\mathcal{C} = \mathbb{P}_\infty\sigma(u) \cdot \varepsilon(u) + 2b_0 \cdot u, \tag{3.5}$$

with u solution to (2.3) and the polarization tensor $\mathbb{P}_\infty$ given by

$$\mathbb{P}_\infty = -\frac{\lambda + 2\mu}{\lambda + 3\mu}\left(2\mathbb{I} + \frac{\mu - \lambda}{2(\lambda + \mu)}\mathrm{I} \otimes \mathrm{I}\right). \tag{3.6}$$

Finally, the topological derivative $D_T|\Omega|$ reads

$$D_T|\Omega| = 1. \tag{3.7}$$

4. Numerical results

In this section, some numerical experiments are presented to show the effectiveness of the proposed methodology. The minimization problem (2.1) is solved by using a topology optimization algorithm based on the topological derivative together with a level-set domain representation method (Amstutz and Andrä, 2006). The topology optimization problem (2.1) is conveniently rewritten as follows

$$\begin{cases} \underset{\Omega \subset \mathcal{D}}{\text{Minimize}}\ J^\alpha(\Omega) := \dfrac{J(\Omega)}{J(\mathcal{D})} + \alpha\dfrac{|\mathcal{D}|}{|\Omega|}, \\ \text{Subject to } |\Omega| \leq M, \end{cases} \tag{4.1}$$

where $J(\Omega) = \mathcal{C}(u)$ and $J(\mathcal{D}) = \mathcal{C}(u_0)$, with u and u_0 solutions to (2.3) for $\Omega \subset \mathcal{D}$ and $\Omega \equiv \mathcal{D}$, respectively. The quantities $J(\Omega)/J(\mathcal{D})$ and $|\Omega|/|\mathcal{D}|$ are referred to as *relative compliance* and *volume fraction*, respectively. A simple linear penalization method is used for imposing the volume constraint given by $|\Omega| \leq M$. For more sophisticated topological-derivative-based methods with volume constraint we refer the reader to the paper by Campeão et al. (2014), for instance. Therefore, for the sake of simplicity, we describe the algorithm used to minimize $J^\alpha(\Omega)$ with respect to $\Omega \subset \mathcal{D}$. The topological derivative of $J^\alpha(\Omega)$ is denoted as $D_T J^\alpha(x)$. A locally sufficient optimality condition, under the considered class of domain perturbation given by circular inclusions, can be stated as (Amstutz, 2011):

$$D_T J^\alpha(x) > 0 \quad \forall x \in \mathcal{D}. \tag{4.2}$$

Let us introduce a level-set domain representation function $\psi \in L^2(\mathcal{D})$ of the form:

$$\Omega = \{\psi(x) < 0, \text{ for } x \in \mathcal{D}\}, \tag{4.3}$$

$$\mathcal{D} \setminus \overline{\Omega} = \{\psi(x) > 0, \text{ for } x \in \mathcal{D}\}, \tag{4.4}$$

where ψ vanishes on the interface $\partial\Omega$. We define the quantity

$$g(x) := \begin{cases} -D_T J^\alpha(x), & \text{if } \psi(x) < 0, \\ +D_T J^\alpha(x), & \text{if } \psi(x) > 0, \end{cases} \tag{4.5}$$

allowing for rewriting the condition (4.2) in the following equivalent form

$$\begin{cases} g(x) < 0, & \text{if } \psi(x) < 0, \\ g(x) > 0, & \text{if } \psi(x) > 0. \end{cases} \tag{4.6}$$

Note that (4.6) is satisfied whenever quantity g coincides with level-set function ψ up to a strictly positive number. Thus, the basic idea consists in finding a fixed point satisfying the following condition

$$\tau > 0 : g = \tau\psi. \tag{4.7}$$

Therefore,

$$\theta := \arccos\left[\frac{\langle g, \psi\rangle_{L^2(\mathcal{D})}}{\|g\|_{L^2(\mathcal{D})}\|\psi\|_{L^2(\mathcal{D})}}\right] = 0, \tag{4.8}$$

which shall be used as optimality condition in the topology design algorithm, where θ is the angle between the functions g and ψ in $L^2(\mathcal{D})$. Note that there is a lack of sufficient optimality conditions for such shape optimization problems (Amstutz and Van Goethem, 2012), so that only a local minimum can be ensured.

Let us now explain the algorithm. We first choose an initial level-set function $\psi_0 \in L^2(\mathcal{D})$. In particular, a detailed explanation on the numerical discretization of the level-set function can be found in the original paper by Amstutz and Andrä (2006). In a generic iteration i, we compute function g_i associated with the level-set function $\psi_i \in L^2(\mathcal{D})$. Thus, the new level-set function ψ_{i+1} is updated according to the following linear combination between the functions g_i and ψ_i, explicitly given by

$$\psi_{i+1} = \frac{1}{\sin\theta_i}\left[\sin((1-w)\theta_i)\psi_i + \sin(w\theta_i)\frac{g_i}{\|g_i\|_{L^2(\mathcal{D})}}\right], \tag{4.9}$$

where θ_i is the angle between g_i and ψ_i according to (4.8), and w is a step size determined by a line-search performed in order to decrease the value of the objective function J_i^α associated with ψ_i. The step size w is chosen at first as 1 and it is decreasing accordingly to $w \leftarrow w/2$ until the condition $J_i^\alpha < J_{i-1}^\alpha$ is fulfilled. The process ends when the condition $\theta_i \leq \epsilon_\theta$ is satisfied at some iteration, where ϵ_θ is a given small numerical tolerance. If at some iteration the line-search step size w is found to be smaller than a given numerical tolerance $\epsilon_w > 0$ and the local optimality condition is not satisfied, namely $\theta_i > \epsilon_\theta$, then a mesh refinement of the hold-all domain $\mathcal{D}$ is carried out and the iterative process is continued. The above procedure written in the form of a pseudo-code format is described by Lopes et al. (2015).

In all numerical examples, the stopping criterion and the optimality threshold are given respectively by $\epsilon_w = 10^{-3}$ and $\epsilon_\theta = 1^\circ$. The current volume fraction is denoted by $V(\%)$ and we consider a tolerance of $\pm 1\%$ in the volume constraint. The angle θ has converged to a value smaller than 1°, namely, the local optimality condition has been satisfied in all cases. Furthermore, the mechanical problem is discretized into linear triangular finite elements and three steps of uniform mesh refinement were performed during the iterative process in order to fulfill the optimality condition, except when explicitly indicated. Also, the following material properties are assumed (Xu et al., 2013): Young's modulus $E =$

$210,000\ MPa$ and Poisson ratio $\nu = 0.3$. Finally, the traction q and the body force b are defined as

$$q = \kappa q_0 \quad \text{and} \quad b = \gamma b_0, \quad \text{with} \quad b_0 = -\rho_0 g e_2, \tag{4.10}$$

where $e_i,\ i = 1, 2$ denotes the canonical basis of $\mathbb{R}^2$, γ is given by (2.7), $\rho_0 = 7.85 \times 10^3\ kg/m^3$, $g = 10 m/s^2$ and $0 \leq \kappa \leq 1$ is a weight parameter.

The role of the regularizing parameter α is discussed through the benchmark from Section 4.1, in which only self-weight loading is considered. Sections 4.2, 4.3 and 4.4 show different features of the topological derivative method itself in solving the original (non-regularized) problem. Finally, Section 4.5 presents a last experiment which takes into account both the regularizing parameter α and the loading factor κ.

4.1. **Experiment 1.** In this example, the hold-all domain $\mathcal{D}$ is given by a rectangle of dimensions $20 \times 10\ m^2$ as shown in Figure 3. We consider symmetry condition with respect to the vertical axis and the problem is discretized with an initial mesh containing $1,600$ elements and 841 nodes. At the end of the iterative process, the mesh contains $102,400$ elements and $51,521$ nodes.

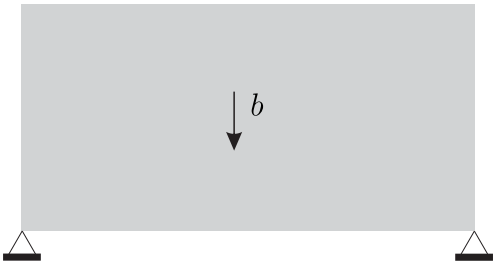

FIGURE 3. Experiment 1: Initial domain and boundary conditions.

In order to observe the role of the regularizing parameter in the case where only self-weight loading is considered ($\kappa = 0$), we take it in the interval $0 \leq \alpha \leq 2.3$ to produce the graph from Figure 4, showing the behavior of the relative compliance and the volume fraction of the structure with respect the regularizing parameter α. For $\alpha = 0$ the volume fraction converges to zero, as expected. On the other hand, the volume fraction goes to 100% for $\alpha = 2.3$. In between, namely $0 < \alpha < 2.3$, a family of non-trivial solutions is obtained.

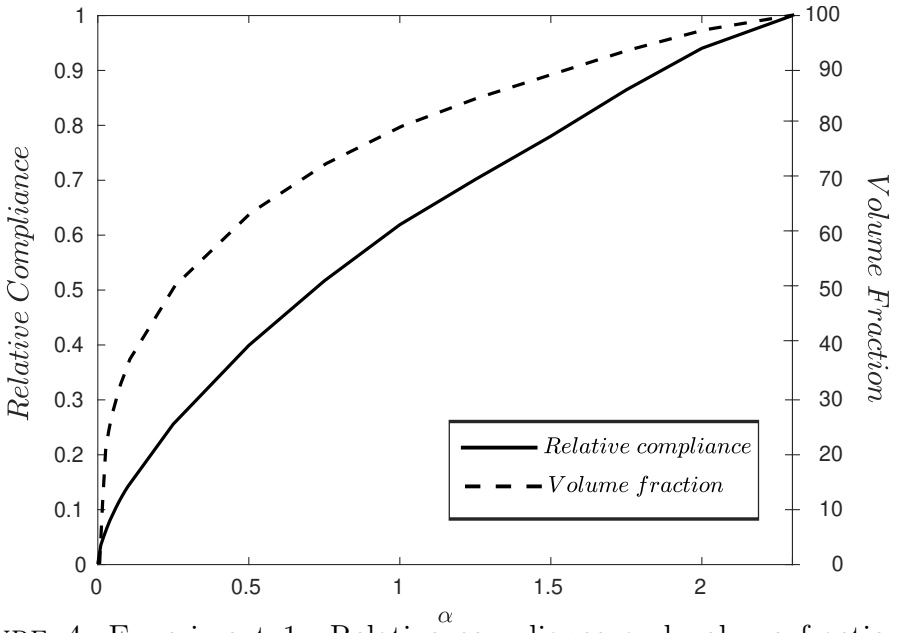

FIGURE 4. Experiment 1: Relative compliance and volume fraction for different values of α.

As shown in Figure 4, by setting $\alpha = 2.3$ we have a volume fraction $V = 100\%$. Let us impose a volume constraint $M = 0.5\,|\mathcal{D}|$ to obtain a new solution with volume fraction $V \approx 50\%$. Now we can compare the constrained solution with the unconstrained one obtained with $\alpha = 0.245$, corresponding to the same volume fraction. Both of them converge to the same solution up to a small numerical tolerance, with volume fractions $V \approx 50\%$. Figure 5 presents the obtained results. Table 1 shows the values of relative compliance, volume fraction and number of iterations at the end of the iterative process for both cases. As expected, the constrained case needs more iterations to converge than the unconstrained one.

(a) (b)

FIGURE 5. Experiment 1: Obtained results for the unconstrained case (a) with $\alpha = 0.245$ and for the constrained case (b) with $\alpha = 2.3$ and $M = 0.5\,|\mathcal{D}|$.

TABLE 1. Experiment 1: Quantitative results obtained at the end of the iterative process for the unconstrained case with $\alpha = 0.245$ and for the constrained case with $\alpha = 2.3$ and $M = 0.5\,|\mathcal{D}|$.

	Unconstrained Case	Constrained Case
Relative Compliance	0.25233	0.25284
Volume Fraction (%)	50.306	50.389
Number of Iterations	19	102

4.2. **Experiment 2.** In this example, both external and body forces are taken into account. The body force is given by (4.10), whereas the external force is defined as

$$q_0 = \int_{\mathcal{D}} b_0 \, d\mathcal{D}. \tag{4.11}$$

The hold-all domain $\mathcal{D}$ is a rectangle of dimensions $40 \times 10\ m^2$. We consider symmetry condition with respect to the vertical axis and the problem is discretized with an initial mesh containing $3,200$ elements and $1,661$ nodes, whereas the final mesh contains $204,800$ elements and $102,881$ nodes.

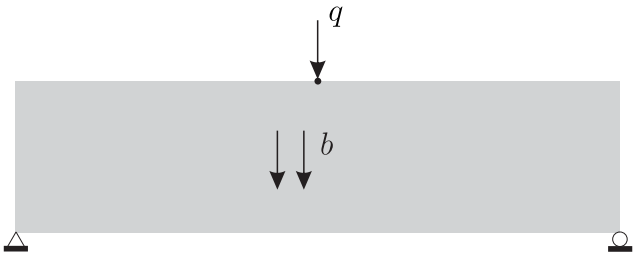

FIGURE 6. Experiment 2: Initial domain and boundary conditions.

First, we set $\alpha = 0$ and choose the loading factor $\kappa \in \{0.1, 0.2, 0.3, 0.4\}$. Figure 7 presents the obtained results for the unconstrained case. We observe that the volume fraction increases with the loading factor, as expected. Table 2 shows the values of relative compliance, volume fraction, and number of iterations at the end of the iterative process for all cases.

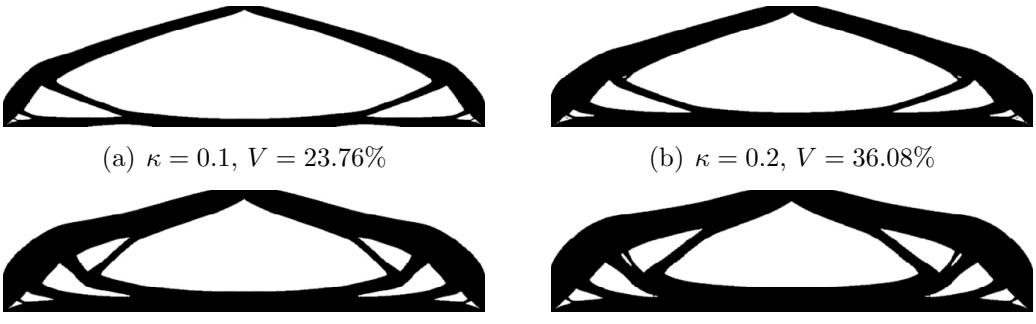

(a) $\kappa = 0.1$, $V = 23.76\%$ (b) $\kappa = 0.2$, $V = 36.08\%$

(c) $\kappa = 0.3$, $V = 45.74\%$ (d) $\kappa = 0.4$, $V = 53.13\%$

FIGURE 7. Experiment 2: Obtained results for the unconstrained case with $\alpha = 0$.

TABLE 2. Experiment 2: Quantitative results obtained at the end of the iterative process for the unconstrained case with $\alpha = 0$.

Loading Factor κ	0.1	0.2	0.3	0.4
Relative Compliance	0.24414	0.43145	0.5729	0.67367
Volume Fraction (%)	23.76	36.08	45.74	53.13
Number of Iterations	45	36	26	21

Now, a volume constraint $M = 0.4\,|\mathcal{D}|$ is imposed. We set $\kappa \in \{0.4, 0.6, 0.8, 1.0\}$ and choose $\alpha = 0$. Figure 8 presents the obtained results for the constrained case.

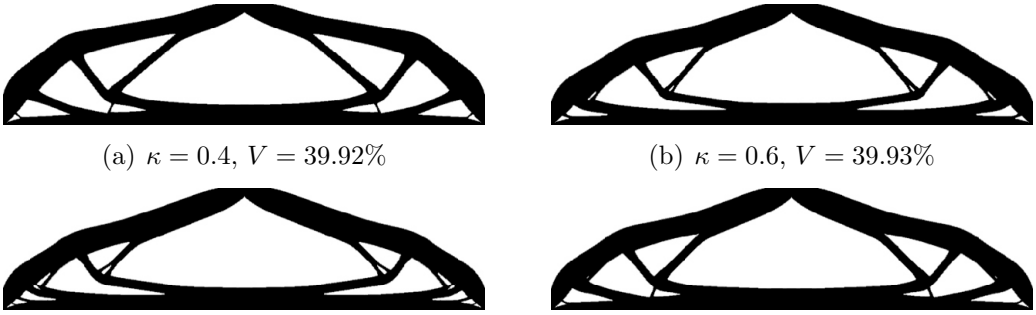

(a) $\kappa = 0.4$, $V = 39.92\%$ (b) $\kappa = 0.6$, $V = 39.93\%$

(c) $\kappa = 0.8$, $V = 40.26\%$ (d) $\kappa = 1$, $V = 40.05\%$

FIGURE 8. Experiment 2: Obtained results for the constrained case with $\alpha = 0$ and $M = 0.4\,|\mathcal{D}|$.

The values of relative compliance, volume fraction, and number of iterations at the end of the iterative process for all cases are shown in Table 3. Note that all the structures satisfies the required volume fraction up to a small numerical tolerance.

TABLE 3. Experiment 2: Quantitative results obtained at the end of the iterative process for the constrained case with $\alpha = 0$ and $M = 0.4\,|\mathcal{D}|$.

Loading Factor κ	0.4	0.6	0.8	1.0
Relative Compliance	0.65251	0.83827	0.98358	1.0618
Volume Fraction (%)	39.92	39.93	40.26	40.05
Number of Iterations	39	32	37	32

Finally, for the sake of comparison, in Figure 9, we present the obtained result free of self-weight loading, namely, for $b = 0$. In particular, we set $\alpha = 0$, $\kappa = 1$ and $M = 0.4\,|\mathcal{D}|$. This result was obtained after 31 iterations with final volume fraction $V = 40.87\%$. In Section 4.4, we also present an example in which the self-weight loading is initially neglected, and later on the body force is taken into account again, allowing for comparing both results. In this case, the resulting topologies are completely different from each other.

FIGURE 9. Experiment 2: Obtained result free of self-weight loading ($b = 0$), with $\alpha = 0$, $\kappa = 1$ and $M = 0.4\,|\mathcal{D}|$.

4.3. **Experiment 3.** Let us consider again Experiment 2 but with

$$q_0 = -\int_{\mathcal{D}} b_0 \, d\mathcal{D}, \tag{4.12}$$

as shown in Figure 10. In particular, a self-equilibrated problem is considered by setting $\kappa = 1.0$.

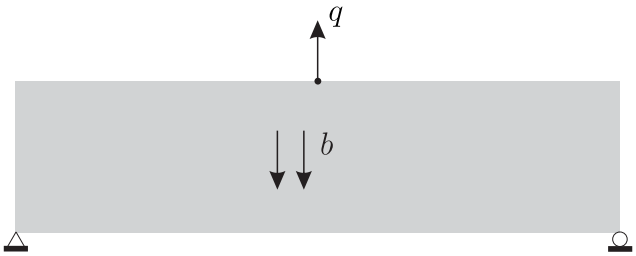

FIGURE 10. Experiment 3: Initial domain and boundary conditions.

In this experiment, a volume constraint $M = 0.5\,|\mathcal{D}|$ is imposed. We consider again $\alpha = 0$. The result, shown in Figure 11, was obtained after 34 iterations with volume fraction $V = 49.99\%$.

FIGURE 11. Experiment 3: Obtained result for the constrained case with $\alpha = 0$, $\kappa = 1.0$ and $M = 0.5\,|\mathcal{D}|$.

4.4. **Experiment 4.** In this example, the hold-all domain $\mathcal{D}$ is given by a square of dimensions $10 \times 10\ m^2$, which is submitted to both external and body forces. See sketch from Figure 12. In contrast to the former examples, the traction q is acting in the horizontal direction, orthogonal to the body force b. The problem is discretized with an initial mesh containing $1,600$ elements and 841 nodes, whereas the final mesh has $102,400$ elements and $51,521$ nodes. Finally, we set $\alpha = 0$, $\kappa = 0.4$ and $M = 0.4\,|\mathcal{D}|$. Note that from this choice of parameters, the external traction and the total weight of the structure shall have the same magnitude at the end of the iterative process.

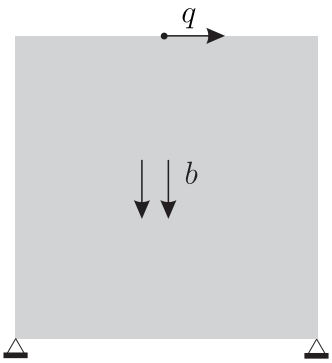

FIGURE 12. Experiment 4: Initial domain and boundary conditions.

For the sake of comparison, we first consider the case free of self-weight loading and later on we present the result by taking into account the body force. In particular, we start by neglecting the weight of the structure, namely, the body force is set as $b = 0$. The final topology is presented in Figure 13(a), which has been obtained after 14 iterations, with final volume fraction $V = 39.94\%$. Then, the self-weight of the structure is taken into account as in the former experiments. The final topology can be seen in Figure 13(b), which has been obtained after 18 iterations, with final volume fraction $V = 40.78\%$. Note that in this case the resulting topologies reported in Figure 13 are completely different from each other.

(a) $b = 0$, $V = 39.94\%$ (b) $b \neq 0$, $V = 40.78\%$

FIGURE 13. Experiment 4: Obtained results for $\alpha = 0$, $\kappa = 0.4$ and $M = 0.4\,|\mathcal{D}|$.

4.5. **Experiment 5.** Let us consider the design of a tower by taking into account both external and body forces. The hold-all domain $\mathcal{D}$ is given by a rectangle of dimensions 120×300 m^2, as shown in Figure 14(a) and the external force is given as (4.11). We consider symmetry condition with respect to the vertical axis, and the problem is discretized with an initial mesh containing $8,000$ elements and $4,121$ nodes. Four steps of uniform mesh refinement have been performed during the optimization process, leading to a final mesh with $2,048,000$ elements and $1,025,921$ nodes. In this experiment, we choose $\alpha = 0.01$ and load factor $\kappa = 0.1$. Finally, a volume constraint of $M = 0.21\,|\mathcal{D}|$ is imposed. The result, shown in Figure 14(b), was obtained after 50 iterations with final volume fraction $V = 21.62\%$. The history of the shape functional and the volume fraction during the iterative process is presented in Figure 15.

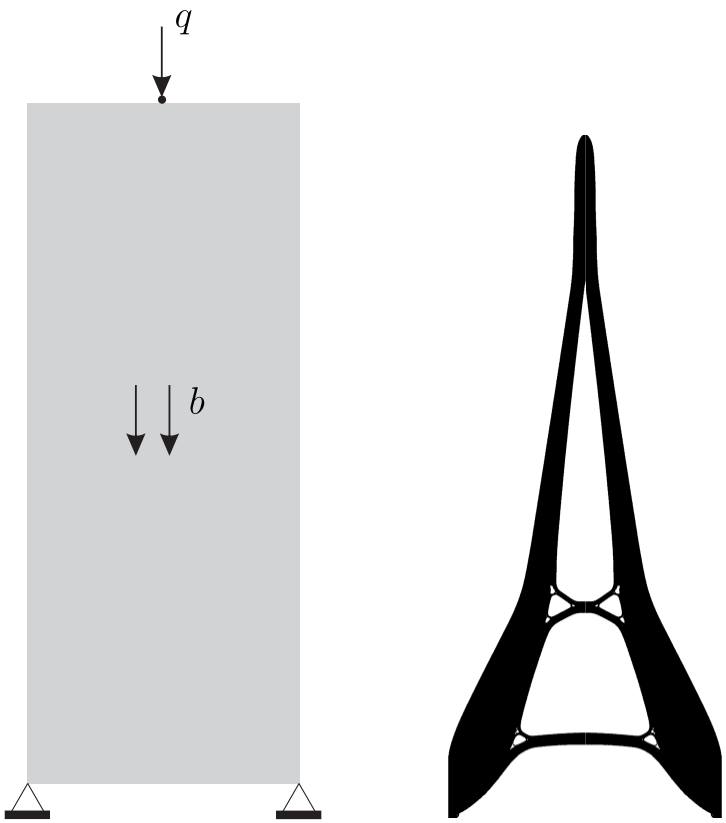

(a) (b)

FIGURE 14. Experiment 5: Initial domain and boundary conditions (a), and obtained result for the constrained case (b) with $\alpha = 0.01$, $\kappa = 0.1$ and $M = 0.21\,|\mathcal{D}|$.

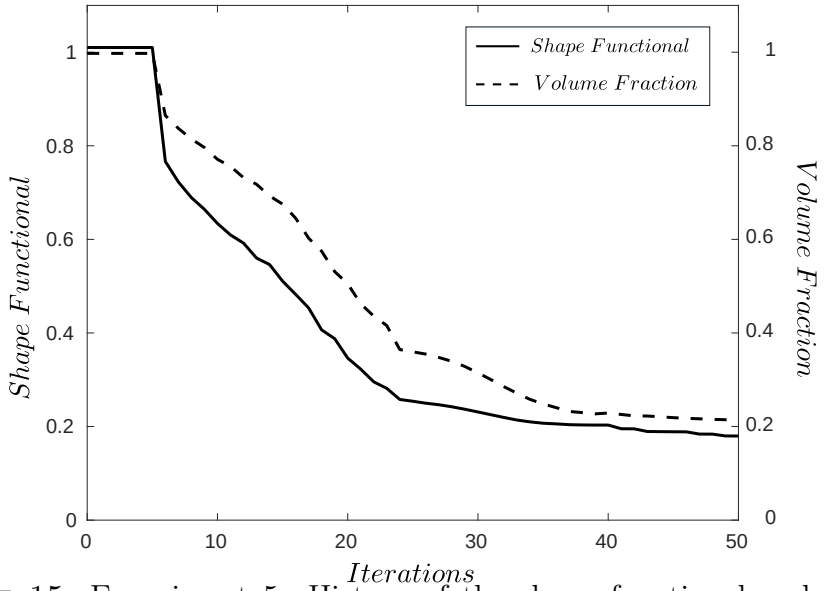

FIGURE 15. Experiment 5: History of the shape functional and volume fraction during the iterative process.

5. Conclusions

In this paper, the topology optimization of structures subject to self-weight loading has been revisited. We have observed that the standard formulation based on compliance minimization under volume constraint becomes inappropriate when self-weight loading is dominant, as pointed out by Bruyneel and Duysinx (2005). Therefore, we have introduced a regularizing term to the compliance-based minimization problem that allows for imposing any feasible volume constraint, leading to satisfactory results by avoiding trivial solutions and convergence issues. The original formulation is recovered once the regularizing parameter vanishes. The resulting topology optimization problem has been solved with the help of the topological derivative method leading to a 0-1 topology design algorithm, which seems to be crucial when the self-weight load becomes dominant. Finally, several numerical experiments were presented, showing the effectiveness of the proposed approach in solving a structural topology optimization problem under self-weight loading.

Acknowledgements

This research was financed in part by the Coordenação de Aperfeiçoamento de Pessoal de Nível Superior - Brasil (CAPES) - Finance Code 001. It was also partly supported by CNPq (Brazilian Research Council) and FAPERJ (Research Foundation of the State of Rio de Janeiro). These supports are gratefully acknowledged. Finally, we would like to thanks G. H. Paulino for the helpful discussion during the earlier versions of this paper.

Conflict of interest

The authors declare that they have no conflict of interest.

Replication of results

The authors are agreeable to share the codes and details of results with those who contact them.

References

S. Amstutz. Analysis of a level set method for topology optimization. *Optimization Methods and Software*, 26(4-5):555–573, 2011.

S. Amstutz and H. Andrä. A new algorithm for topology optimization using a level-set method. *Journal of Computational Physics*, 216(2):573–588, 2006.

S. Amstutz and N. Van Goethem. Topology optimization methods with gradient-free perimeter approximation. *Interfaces and Free Boundaries*, 14(3):401–430, 2012.

R. Ansola, J. Canales, and J. A. Tárrago. An efficient sensitivity computation strategy for the evolutionary structural optimization (eso) of continuum structures subjected to self-weight loads. *Finite Elements in Analysis and Design*, 42:1220–1230, 2006.

M. Bruyneel and P. Duysinx. Note on topology optimization of continuum structures including self-weight. *Structural and Multidisciplinary Optimization*, 29:245–256, 2005.

D. E. Campeão, S. M. Giusti, and A. A. Novotny. Topology design of plates consedering different volume control methods. *Engineering Computations*, 31(5):826–842, 2014.

L. Félix, A. A. Gomes, and A. Suleman. Topology optimization of the internal structure of an aircraft wing subjected to self-weight load. *Engineering Optimization*, 52(7): 1119–1135, 2020.

E. Holmberg, C.J. Thore, and A. Klarbring. Worst-case topology optimization of self-weight loaded structures using semi-definite programming. *Structural and Multidisciplinary Optimization*, 52:915–928, 2015.

X. Huang and Y.M. Xie. Evolutionary topology optimization of continuum structures including design-dependent self-weight loads. *Finite Elements in Analysis and Design*, 47:942–948, 2011.

C. G. Lopes, R. B. Santos, and A. A. Novotny. Topological derivative-based topology optimization of structures subject to multiple load-cases. *Latin American Journal of Solids and Structures*, 12:834–860, 2015.

A. A. Novotny and J. Sokołowski. *Topological derivatives in shape optimization*. Interaction of Mechanics and Mathematics. Springer-Verlag, Berlin, Heidelberg, 2013. doi: 10.1007/978-3-642-35245-4.

A. A. Novotny and J. Sokołowski. *An introduction to the topological derivative method*. Springer Briefs in Mathematics. Springer Nature Switzerland, 2020.

A. A. Novotny, J. Sokołowski, and A. Żochowski. *Applications of the topological derivative method*. Studies in Systems, Decision and Control. Springer Nature Switzerland, 2019. doi: 10.1007/978-3-030-05432-8.

S. Turteltaub and P. Washabaugh. Optimal distribution of material properties for an elastic continuum with structure-dependent body force. *International Journal of Solids and Strutures*, 36:4587–4608, 1999.

H. Xu, L. Guan, X. Chen, and L. Wang. Guide-weight method for topology optimization of continuum structures including body forces. *Finite Elements in Analysis and Design*, 75:38–49, 2013.

(A.A. Novotny) Laboratório Nacional de Computação Científica LNCC/MCT, Coordenação de Métodos Matemáticos e Computacionais, Av. Getúlio Vargas 333, 25651-075 Petrópolis - RJ, Brasil

Email address: novotny@lncc.br

(C.G. Lopes) Instituto Federal de Sergipe, Rod. Juscelino Kubitschek s/n, 49680-000 Nossa Senhora da Glória - SE, Brasil

Email address: lopesgcinthia@gmail.com

(R.B. Santos) Universidade Federal do Rio Grande do Norte, Departamento de Matemática, Av. Salgado Filho 3000, 59078-970 Natal - RN, Brasil

Email address: renathabat@gmail.com